Available online at www.sciencedirect.com

SCIENCE DIRECT®

International Journal of Mass Spectrometry 239 (2004) 57–65

International Journal of Mass Spectrometry

www.elsevier.com/locate/ijms

# A selected ion flow tube, SIFT, study of the ion chemistry of $H_3O^+$, $NO^+$ and $O_2^{+\bullet}$ ions with several nitroalkanes in the presence of water vapour

Kseniya Dryahina, Miroslav Polášek, Patrik Španěl*

*J. Heyrovský Institute of Physical Chemistry, Academy of Sciences of the Czech Republic,*
*Dolejškova 3, 18223 Prague 8, Czech Republic*

Received 17 August 2004; accepted 22 September 2004
Available online 28 October 2004

## Abstract

We have carried out a selected ion flow tube (SIFT) study of the reactions of $H_3O^+$, $NO^+$ and $O_2^{+\bullet}$ with the following six nitroalkanes: nitromethane, nitroethane, 1-nitropropane, 2-nitropropane, 1-nitrobutane and 2-methyl-2-nitropropane. The primary purpose of this work was to extend the kinetics database to allow these compounds, M, to be analysed in air by selected ion flow tube mass spectrometry, SIFT–MS. Some nitroalkanes are used as industrial solvents and some are component of agricultural agents that are known health hazards. The initial step in all the $H_3O^+$ reactions is exothermic proton transfer to produce $MH^+$ ions, which are seen to be the only products for the two smallest nitroalkanes, but for the isomers of nitropropane and nitrobutane, fragmentation of the nascent $MH^+$ ions occurs. $NO^+$ reacts with the four smallest compounds via association resulting in $NO^+M$ product ions, whilst for the isomers of nitrobutane the $C_4H_9^+$ hydrocarbon ion is produced. The reaction of $O_2^{+\bullet}$ with nitromethane proceeds via charge transfer giving $M^{+\bullet}$ as the major product, whilst the $O_2^{+\bullet}$ reactions with all the remaining nitroalkanes in this study lead to a single hydrocarbon ion product $C_nH_{2n+1}^+$. The secondary chemistry of the ion products with $H_2O$ and with M, which is relevant to SIFT–MS applications, is fully described, with the interesting finding that water cluster ions of the kind $MH^+(H_2O)_3$ containing three water molecules are formed at 300 K. The mechanisms of the reactions are described with the aid of ab initio calculations of the ion energetics that were not previously available for some of the ions involved in the chemistry.

*Keywords:* SIFT; Nitropropane; Nitromethane; SIFT–MS

## 1. Introduction

Nitroalkanes are commonly used as solvents in industrial construction and maintenance, printing, highway maintenance and food packaging. They have been widely used as chemical intermediates, industrial solvents, and as components of inks, paints, varnishes and other coatings [1]. Potential occupational exposure to nitro compounds occurs during their manufacture and use. Nitromethane, along with other nitroalkanes, has been detected in cigarette smoke [2]. Nitromethane and 2-nitropropane are considered to be carcinogenic to humans and animals [3,4]. High concentrations of nitroalkanes (above 600 ppm) are acutely toxic and have produced industrial fatalities [5]. Occupational exposure limits set by the US Department of Labour are 100 ppm for nitromethane and nitroethane and 25 ppm for both isomers of nitropropane [6]. Selected ion flow tube (SIFT)–MS [7] has the potential for accurate on-line real time measurement and monitoring of concentrations of these nitroalkanes in air.

SIFT–MS may also be feasible analytical method for biological monitoring via breath analysis of the exposure of workers to the most widely used nitroalkane, 2-nitropropane. Human uptake of nitroalkanes occurs mainly through the lungs. In experimental studies on animals (rats) [5] it has been shown that 2-nitropropane is not only rapidly absorbed via the lungs but also via the peritoneal cavity and the gastrointestinal tract; however, there is no satisfactory information on absorption via the skin. 2-Nitropropane is not retained in the body for more than a few hours, since it is rapidly metabolised,

---

* Corresponding author. Tel.: +420 2 6605 2112; fax: +420 2 858 2307.
*E-mail address:* spanel@seznam.cz (P. Španěl).

1387-3806/$ – see front matter © 2004 Elsevier B.V. All rights reserved.
doi:10.1016/j.ijms.2004.09.007

mainly to acetone, nitrite salts and possibly some isopropyl alcohol [8]. These metabolites and 2-nitropropane are then rapidly lost from the body by further metabolic transformation, exhalation and excretion [5].

The data also may be of some relevance to atmospheric ion chemistry. In situ measurements of the ion composition of the atmosphere indicate that $CH_3NO_2$ is also present as a component of complex hydrated $H_3O^+$ based clusters [9].

In order to establish the library of kinetic data and to understand the trends of reactivity of the common SIFT–MS precursor ions $H_3O^+$, $NO^+$, $O_2^{+\bullet}$, a series of studies of the reaction of these ions with different classes of molecules has been carried out; see the recent studies of the reactions of diols and the references there in [10]. The objective of the present study is to extend this library of data by providing information on the trends of reactivity of several nitroalkanes with the SIFT–MS precursor ions. As the information on proton affinities (PAs) is not available for all the nitroalkanes included, the study was complemented by their ab initio calculations. Details of the reaction mechanisms involving fragmentation were elucidated by information from parallel study using collisionally activated dissociation (CAD) in a sector mass spectrometer.

Protonated parent molecules that are produced in the primary reactions of $H_3O^+$ with small molecules can bind one or more water molecules under the typical conditions of the SIFT experiments, viz. helium carrier gas, temperature 300 K, pressure 100 Pa. Notable exception are protonated hydrocarbons that do not associate efficiently with $H_2O$ under these SIFT conditions [11]. The maximum number of bound water molecules is characteristic of the different classes of compounds. Thus ketones, ethers and esters typically bind only a single water molecule [12], but aldehydes [13], alcohols [14] and carboxylic acids [15] can bind two $H_2O$ molecules. The biggest number of added water molecules observed to date in SIFT experiments at 300 K is three for $H_3O^+$ [16] and $CH_3CNH^+$ [17]. As it will be shown later, the protonated nitroalkanes also are seen to add three water molecules.

## 2. Methods

### 2.1. Selected ion flow tube (SIFT)

The well-known SIFT technique for the determination of the rate coefficients and ion product distributions for the reactions of $H_3O^+$, $NO^+$ and $O_2^{+\bullet}$ ions with organic compounds has been described in numerous previous publications [18,19], so it is sufficient here to summarise it as follows. Precursor ions ($H_3O^+$, $NO^+$ and $O_2^{+\bullet}$) are generated in a microwave discharge ion source, mass selected by a quadrupole mass filter and then injected as into helium carrier gas, flowing at a velocity of 170 m/s in the Prague SIFT. The reactant vapours of interest (in these experiments, nitromethane, nitroethane, 1-nitropropane, 2-nitropropane, 1-nitrobutane and 2-methyl-2-nitropropane) are then introduced into the ion swarm/carrier gas where they react with the chosen precursor ion species. Measurement of the absolute flow rates of their neat vapours into the carrier gas of the SIFT instrument, required for determination of absolute rate coefficients [18], cannot be achieved to an accuracy better than 20% due to the surface activity of these compounds. In these circumstances, the established procedure is to measure relative rate coefficients of the $H_3O^+$, $NO^+$ and $O_2^{+\bullet}$ ions with the compound. Thus, the reactant nitroalkane is introduced as its saturated vapour in helium by introducing a small droplet of liquid nitroalkane in a sealed plastic bag, which is then inflated with helium. This helium/nitro compound vapour mixture is then introduced into the helium carrier gas/precursor ion swarm of the SIFT via a flow meter in the usual way. The $H_3O^+$, $NO^+$ and $O_2^{+\bullet}$ ions are injected simultaneously into the carrier gas by switching the injection mass filter to the total ion mode [20].

The relative concentrations of the primary and product ions of the reactions are determined from the count rates recorded by a downstream quadrupole mass spectrometer with a pulse counting single channel electron multiplier detector. This can be operated in the full scan mode (FSM) over a predetermined *m/z* range to obtain a spectrum of the reactant and product ions or in the multi-ion mode (MIM) in which the spectrometer is switched and dwells on selected reactant/product ions as their count rates are determined [20]. The FSM is primarily used to identify the product ions and the MIM is used to accurately determine the rate coefficients and the product ion distributions [20,21]. Primary product branching ratios are determined by extrapolation of the measured ion count rate ratios towards zero reactant flow rate [18].

The relative rate coefficients for the reactions of the three precursor ions with the given molecule are then determined from the slopes of the plots of logarithm of ion count rates against the vapour mixture flow rate. It can be justifiably assumed that the proton transfer reactions of $H_3O^+$ with the nitroalkane compounds are exothermic and proceed at their collisional rates, because the proton affinities of the nitroalkanes exceed the proton affinity of water molecules [22] by >20 kJ/mol [23]. Collisional rate coefficients, $k_c$, for the $H_3O^+$ reactions have been calculated from the polarizabilities and the dipole moments of the reactant nitroalkanes using the parameterised trajectory formulation of Su and Chesnavich [24]. Values of the dipole moments and of the polorizabilities are from [25] with the single exception of 2-nitropropane, the polarizability of which is unknown, but we estimate it to be the same as the polarizability of its isomer 1-nitropropane. The rate coefficients, $k$, for the $NO^+$ and $O_2^{+\bullet}$ reactions are then experimentally derived from the relative decay rates of the three ion species (see the previous successful applications of this procedure, for example, in [12,13]).

In SIFT–MS analyses of moist air samples, it is important to know if any of the product ions, $R^+$, of the analytical reactions undergo association with water molecules [16]. To

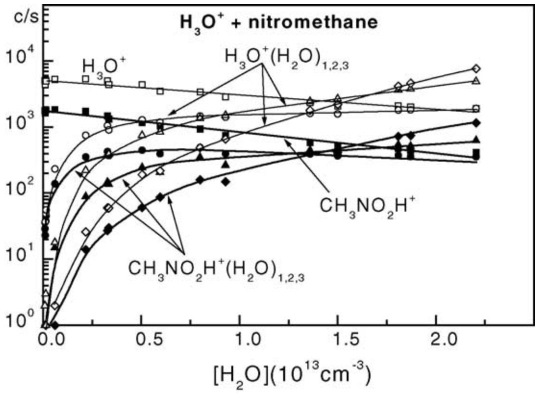

Fig. 1. Experimental SIFT data tracing the ion chemistry that occurs when $H_3O^+$ ions are injected into the helium carrier gas into which a small steady flow of nitromethane and variable flows of water vapour are introduced. The count rates, c/s, for the precursor and product ions indicated are plotted on a semilogarithmic scale as a function of the number density of water molecules $[H_2O]$ in the carrier gas.

investigate this, controlled amounts of an air/water vapour mixture were introduced into the carrier gas whilst monitoring the $R^+$ ions using the MIM mode (see Fig. 1). The rate coefficients for association reactions that occur can be estimated from the dependencies of the $[R^+\cdot H_2O]/[R^+]$ count rate ratio on the $H_2O$ molecule number density in the carrier gas, which is calculated from the distribution of the $H_3O^+$ ions and its hydrates $H_3O^+\cdot(H_2O)_{1,2,3}$. This procedure has been discussed previously in a paper on the influence of humidity on SIFT–MS analyses [16].

### 2.2. *Collisionally activated dissociation (CAD), mass spectrometry*

In order to elucidate mechanisms of the fragmentation observed in the $O_2{}^{+\bullet}$ reactions, additional information was used from collisionally activated dissociation mass spectra recorded on ZAB2-SEQ hybrid tandem mass spectrometer equipped with chemical ionisation (CI) ion source. The ions of interest were generated by self-chemical ionisation (self-CI) using the standard ion source conditions (0.5 mA, 100 eV, 150 °C) at the pressure of $6 \times 10^{-3}$ Pa measured at the ion source diffusion pump intake. The ions were extracted from the ionisation chamber, accelerated to 8 keV, and products of their collisional activation in the first and second field-free regions were analysed using the $B/E$ = const. linked scan and mass-analysed ion kinetic energy (MIKE) scan, respectively. Helium was used as a collision gas.

### 2.3. *Quantum chemical calculations*

Standard ab initio calculations of proton affinities of nitroalkanes were preformed using the Gaussian 98 suite of programs [26]. Geometries were optimised with density functional calculations using Becke's hybrid functional (B3LYP) [27] and the 6-31+G(d,p) basis set. Stationary points were characterized by harmonic frequency calculations as local minima (all frequencies real). The calculated frequencies were scaled by the factor of 0.963 [28] and used to obtain zero-point energy (ZPVE) corrections and enthalpies. For selected species, the geometries were also optimised at the MP2/6-31+G(d,p) level of theory. Improved energies were obtained by single-point calculations at two levels of theory. The first set of energies resulted from B3LYP/6-311+G(3df,2p) calculations. The second set of energies was calculated using the G2(MP2) method [29] consisting of MP2/6-311+G(3df,2p), MP2/6-311G(d,p), and QCISD(T)/6-311G(d,p) calculations that were combined to provide effective QCISD(T)/6-311+G(3df,2p) energies corrected for ZPVE and the number of valence electrons. According to definition, the proton affinity of molecule M is the negative enthalpy change of the hypothetical protonation reaction $H^+ + M \rightarrow MH^+$ at 298 K. Therefore, the geometries of the lowest energy conformers of neutral nitroalkanes and their *O*-protonated ionic counterparts were found and used for accurate single-point energy calculation at two levels of theory (vide supra).

## 3. Results

### 3.1. *Proton affinities of nitroalkanes*

To the best of our knowledge, proton affinities are only available for nitromethane and nitroethane [22]. Since there is also very few theoretical values available [30,31], as a part of the present study we have calculated ab initio the proton affinities of nitroethane, 1-nitropropane, 2-nitropropane, 1-nitrobutane and 2-methyl-2-nitropropane. The results are summarized in Table 1. For the three compounds where previous theoretical or experimental values are available the agreement is within the estimated uncertainty of the theoretical method, ±7 kJ/mol [29].

### 3.2. *Rate coefficients for the $H_3O^+$, $NO^+$ and $O_2{}^{+\bullet}$ reactions*

The calculated collisional rate coefficient, $k_c$, for the reactions of $H_3O^+$ with the nitroalkanes and the derived rate coefficients, $k$, for the corresponding $NO^+$ and $O_2{}^{+\bullet}$ reactions are listed in Table 2. As can be seen, the $k$ values for the $NO^+$ reactions increase with the number of carbon atoms in the nitroalkane molecules. The $k$ values for the $O_2{}^{+\bullet}$ reactions are close to their respective $k_c$ values (within the 20% experimental error). The only significant exception is the reaction of $O_2{}^{+\bullet}$ with nitromethane, the $k$ value being somewhat lower at 0.75 $k_c$.

Previous measurements are available for the reaction of $H_3O^+$ with nitromethane ($k$ reported as $4.1 \pm 1\,cm^3\,s^{-1}$ [32] and $4.11 \pm 1\,cm^3\,s^{-1}$ [33]), agreeing well with our calculated $k_c$.

Table 1
Calculated proton affinities (298 K) of nitroalkanes in kJ/mol

| Molecule | B3LYP/6-31+G(d,p) | B3LYP/6-311+G(3df,2p) | G2(MP2)[a] | Previous[c] |
|---|---|---|---|---|
| Nitromethane | 740 | 745 | 747[b] | 754.6 |
| Nitroethane | 761 | 767 | 766 | 765.7 |
| 1-Nitropropane | 769 | 774 | 772 | |
| 2-Nitropropane | 774 | 780 | 778 | 777.1 |
| 1-Nitrobutane | 773 | 779 | 776 | |
| 2-Methyl-2-nitropropane | 788 | 793 | 790 | |

[a] Uncertainty estimated as mean average deviation is ±7 kJ/mol [29].

[b] Value taken from [31].

[c] The values of proton affinities for nitromethane and nitroethane are from [22,33] and that for 2-nitropropane is from [30].

Table 2
Rate coefficients for the reactions of $H_3O^+$, $NO^+$ and $O_2^{+\bullet}$ with the nitroalkanes indicated

| Molecule | $M$ (Da) | $\alpha$[a] ($10^{-24}$ cm$^3$) | $\mu$ (D) | $H_3O^+$ [$k_c$] ($10^{-9}$ cm$^3$ s$^{-1}$) | $NO^+$ $k$[b] [$k_c$] ($10^{-9}$ cm$^3$ s$^{-1}$) | $O_2^{+\bullet}$ $k$[b] [$k_c$] ($10^{-9}$ cm$^3$ s$^{-1}$) |
|---|---|---|---|---|---|---|
| Nitromethane | 61 | 7.37 | 3.46 | [4.6] | 0.4 [3.9] | 2.9 [3.8] |
| Nitroethane | 75 | 9.63 | 3.65 | [4.8] | 2.4 [4.0] | 4.6 [3.9] |
| 1-Nitropropane | 89 | 8.5 | 3.66 | [4.6] | 2.5 [3.9] | 3.6 [3.8] |
| 2-Nitropropane | 89 | *8.5 ± 1* | 3.73 | [4.7] | 2.6 [3.9] | 3.3 [3.8] |
| 1-Nitrobutane | 103 | 10.4 | 3.59 | [4.6] | 3.4 [3.9] | 4.4 [3.8] |
| 2-Methyl-2-nitropropane | 103 | 10.3 | 3.71 | [4.7] | 4.2 [3.9] | 4.2 [3.8] |

Also given are their molecular weights, $M$, in Daltons, Da, their polarisabilities, $\alpha$, in units of $10^{-24}$ cm$^3$ and their permanent dipole moments, $\mu$ in Debye, D. The collisional rate coefficients, $k_c$, calculated using the parameterised trajectory formulation of Su and Chesnavich [24] are given in square brackets.

[a] The known $\alpha$ and $\mu$ values [25] are shown in regular type. The estimated $\alpha$ value is shown in italic.

[b] The rate coefficients, $k$, for the $NO^+$ and $O_2^{+\bullet}$ reactions are experimentally derived by the procedure described in Section 2. The absolute and relative uncertainties in these calculated rate coefficients are ±30% and ±15%, respectively.

The products of the reactions and their percentage (in parenthesis) are given in Table 3 together with the known ionisation energies [34] of the nitroalkanes. The trends in reactivity will be discussed briefly in the following subsections.

### 3.3. The $H_3O^+$ reactions

These reactions proceed initially via the formation of a nascent protonated parent molecule, $MH^+$, and this is the only observed product ion for the nitromethane and nitroethane reactions. Partial fragmentation of the nascent $MH^+$ ions occurs for both isomers of nitropropane leading to the formation of the $C_3H_7O^+$ ion; similarly, both isomers of nitrobutane lead to $C_4H_9{}^+$ ions (see Table 3).

There is an obvious difference in the products of the reaction of 1-nitropropane and 2-nitropropane. The reaction of 1-nitrpropane proceeds thus:

$$H_3O^+ + C_3H_7NO_2 \rightarrow C_3H_7NO_2 \cdot H^+ + H_2O; 95\% \quad (1a)$$

$$H_3O^+ + C_3H_7NO_2 \rightarrow C_2H_5CHOH^+ + (HNO + H_2O); 5\% \quad (1b)$$

Here the major product is the protonated parent molecule. Both reactions (1a) and (1b) are exothermic. The reaction exothermicities of reactions (1a) and (1b) calculated at the G2(MP2) level of theory are $-\Delta_r H_{298} = 84$ and 46 kJ/mol respectively. The latter exothermicity is in relatively good agreement with value of 60 kJ/mol calculated for the $C_2H_5CHOH^+$ product structure using data from [35] (see Scheme 1). Note that the identity of the neutral products cannot be directly determined using SIFT, thus we always list the

Table 3
Primary product ions and their percentage (in parenthesis) for the reactions of $H_3O^+$, $NO^+$ and $O_2^{+\bullet}$ with the nitroalkanes indicated

| Molecule | IE (eV)[a] | Productions | | |
|---|---|---|---|---|
| | | $H_3O^+$ | $NO^+$ | $O_2^{+\bullet}$ |
| Nitromethane $CH_3NO_2$ | 11.08 | $CH_3NO_2{\cdot}H^+$ (100) | $CH_3NO_2{\cdot}NO^+$ (100) | $CH_3NO_2{}^+$ (90); $NO^+$ (10) |
| Nitroethane $C_2H_5NO_2$ | 10.90 | $C_2H_5NO_2{\cdot}H^+$ (100) | $C_2H_5NO_2{\cdot}NO^+$ (100) | $C_2H_5{}^+$ (100) |
| 1-Nitropropane $C_3H_7NO_2$ | 10.78 | $C_3H_7NO_2{\cdot}H^+$ (95); $C_3H_7O^+$ (5) | $C_3H_7NO_2{\cdot}NO^+$ (100) | $C_3H_7{}^+$ (100) |
| 2-Nitropropane $(CH_3)_2CHNO_2$ | 10.74 | $C_3H_7NO_2{\cdot}H^+$ (40); $C_3H_7O^+$ (60) | $C_3H_7NO_2{\cdot}NO^+$ (100) | $C_3H_7{}^+$ (100) |
| 1-Nitrobutane $n$-$C_4H_9NO_2$ | 10.71 | $C_4H_9NO_2{\cdot}H^+$ (90); $C_4H_9{}^+$ (10) | $C_4H_9NO_2{\cdot}NO^+$ (85); $C_4H_9{}^+$ (15) | $C_4H_9{}^+$ (100) |
| 2-Methyl-2-nitropropane $(CH_3)_3CNO_2$ | | $C_4H_9NO_2{\cdot}H^+$ (5); $C_4H_9{}^+$ (95) | $C_4H_9{}^+$ (100) | $C_4H_9{}^+$ (100) |

[a] The values of the ionisation energy are from [47].

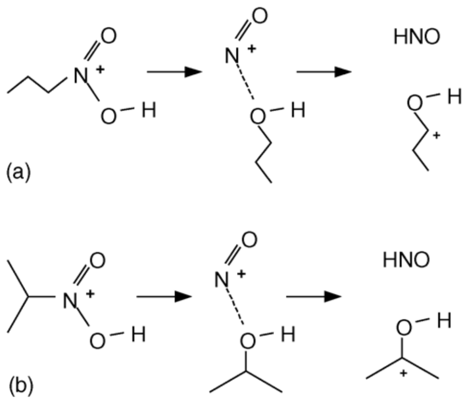

Scheme 1. The nitro-to-nitrite group isomerization by an alkyl cation migration for (a) protonated 1-nitropropane $C_3H_7NO_2{\cdot}H^+$; (b) protonated 2-nitropropane $(CH_3)_2CHNO_2{\cdot}H^+$.

most exothermic neutral products and indicate the possibility of different products by parentheses.

In contrast to this, in the reaction of 2-nitropropane the closed shell $C_3H_7O^+$ fragment is the major product.

$$H_3O^+ + (CH_3)_2CHNO_2 \rightarrow (CH_3)_2CHNO_2 \cdot H^+ + H_2O;\ 40\% \qquad (2a)$$

$$H_3O^+ + (CH_3)_2CHNO_2 \rightarrow (CH_3)_2COH^+ + (HNO + H_2O);\ 60\% \qquad (2b)$$

The exothermicities of (reaction (2a) and (2b) were calculated at the G2 level of theory to be 90 and 93 kJ/mol, respectively. It should be noted that structure of oxygen-protonated propanal, $C_2H_5CHOH^+$, was considered as the product in reaction (2b) whereas protonated acetone, $(CH_3)_2COH^+$, is considered as the product in reaction (2b).

From the mechanistic viewpoint, reactions (1b) and (2b) require some rearrangement of the reactants which allows C–O bonds to form. The nitro-to-nitrite group isomerization (Scheme 1) by an alkyl cation migration may serve as a plausible explanation. However, it cannot be excluded that such rearrangement takes place in a reaction complex with $H_2O$, since methyl cation transfer has already been described in $CH_3NO_2^{+\bullet}$ [36], $CH_3CO^+$ [37] and $CH_3NN^+$ [38] complexes with various atoms and small molecules. Especially in the case of larger systems, after the proton transfer the $H_2O$ leaving the reaction complex could be trapped for a time sufficiently long to be involved in further reaction, a step-wise mechanism, in which the proton transfer (1a) and (2a) takes place as the first step. After the $H_2O$ leaves the reaction complex, the vibrationally excited $C_3H_7NO_2{\cdot}H^+$ rearranges and dissociates unimolecularly to the products (Scheme 1) as it will be discussed in the following section.

It has been found that a methyl group migrating along the $NO_2H$ moiety in protonated nitromethane must proceed over large energy barriers, and so virtually no isomerization was observed during collisional activation [31]. However, migration of larger alkyl cations should be easier due to their higher stability, as was actually observed in protonated nitroethane [39]. Stability of the migrating alkyl cations can be especially important when comparing the reactivity of 1- and 2-nitropropane since the higher stability of a migrating 2-propyl cation can result in higher stabilization of the corresponding transition state. So in the case of 1-nitropropane, the fragmentation shown in Scheme 1a requires migration of a less stable 1-propyl cation over a correspondingly higher energy barrier making the dissociation of $C_3H_7NO_2{\cdot}H^+$ to $C_3H_7O^+$ and HNO much slower. Therefore, protonated 1-nitropropane substantially prevails among the products, whereas in the case of 2-nitropropane, isomerization via the stable 2-propyl cation migration becomes faster, which increases the fraction of $C_3H_7O^+$ and HNO products.

The final step of the proposed reaction mechanism (Scheme 1) involves hydrogen migration from the propyl to the NO group in protonated propyl nitrite. Similar to methyl nitrite [31], protonation of an ether oxygen atom in propyl nitrites leads to the most stable tautomer. Our calculations showed, that $C_3H_7O(H)NO^+$ ions are in fact a complexes of propanols with $NO^+$, as it is indicated by the O–N bond lengths which are 1.98 and 1.95 Å in 1-propyl nitrite and 2-propyl nitrite, respectively. The migration of the most labile α-hydrogen to $NO^+$ is considered to take place producing appropriately $C_3H_7O^+$ ion and a neutral HNO. This, which from the formal point of view is hydride anion abstraction, was found to be the only reaction channel in the 1- and 2-propanol reactions with $NO^+$ [14]. Since the reaction of propanol with $NO^+$ is fast (it proceeds at the collisional rate [14]), the nitro-to-nitrite group rearrangement is most probably the rate-determining step (in the fragmentation shown in Scheme 1) that controls the product distribution.

From the G2(MP2) enthalpies of reactions (1a), (1b), (2a) and (2b) it follows that the dissociation of $C_3H_7NO_2H^+$ to $CH_3CH_2CHOH^+$ and HNO is 38 kJ/mol endothermic and dissociation of $(CH_3)_2CHNO_2{\cdot}H^+$ to $(CH_3)_2COH^+$ and HNO is 3 kJ/mol exothermic. Although the calculation of the isomerization barriers along the reaction path is beyond the scope of this work, from the nature of the SIFT experiment it can be concluded that none of these barriers can exceed the protonation exothermicity reduced by the internal and kinetic energy carried away by the $H_2O$. There are similar differences between the branching ratios of 1-nitrobutane and 2-methyl-2-nitropropane reactions. For 1-nitrobutane the major product is the protonated parent molecule and $C_4H_9{}^+$ is only a minor product:

$$H_3O^+ + C_4H_9NO_2 \rightarrow C_4H_9NO_2 \cdot H^+ + H_2O;\ 90\% \qquad (3a)$$

$$H_3O^+ + C_4H_9NO_2 \rightarrow C_4H_9{}^+ + (HONO + H_2O);\ 10\% \qquad (3b)$$

For the 2-methyl-2-nitropropane reaction the protonated parent molecule is the minor product and $C_4H_9{}^+$ is the major product ion:

$$H_3O^+ + (CH_3)_3CNO_2 \rightarrow (CH_3)_3CNO_2 \cdot H^+ + H_2O; 5\% \quad (4a)$$

$$H_3O^+ + (CH_3)_3CNO_2 \rightarrow C_4H_9{}^+ + (HONO + H_2O); 95\% \quad (4b)$$

The G2(MP2) exothermicity of reaction (3a) is 88 kJ/mol. Estimation of the reaction enthalpy of reaction (3b) is complicated by the fact that no minimum was found on the B3LYP/6-31+G(d,p) potential energy surface (PES) that corresponded to the structure of the 1-butyl cation. This result is in accordance with the study of the $C_4H_9{}^+$ PES carried out by Sieber et al. at the MP2(full)/6-31G** level of theory [40]. Therefore, the exothermicity of reaction (3b) was calculated to be 57 kJ/mol on the assumption that the $C_4H_9{}^+$ cation isomerizes to the most stable *tert*-$C_4H_9{}^+$ structure. For the 2-methyl-2-nitropropane reaction with $H_3O^+$, proton transfer (reaction (4a)) was found to be 102 kJ/mol exothermic, whereas reaction (4b) was estimated to be only 25 kJ/mol exothermic. The latter value is in excellent agreement with a reaction enthalpy of 27 kJ/mol obtained from the available experimental heats of formation [35]. Assuming step-wise reaction mechanisms similar to those discussed in the case of nitropropanes, and combining the energetics of reactions (3a), (3b), (4a) and (4b), the dissociations of $C_4H_9NO_2{\cdot}H^+$ and $(CH_3)_3CNO_2{\cdot}H^+$ to *tert*-$C_4H_9{}^+$ and HONO are 31 and 77 kJ/mol endothermic, respectively.

Mechanistically, the formation of a *tert*-butyl cation in the dissociation of $(CH_3)_3CNO_2{\cdot}H^+$ does not need any rearrangement. Instead, cleavage of the C–N bond leads directly to stable *tert*-$C_4H_9{}^+$ and HONO products. Nevertheless, the rearrangement to protonated *tert*-butyl nitrite according to scheme in Scheme 2 cannot be excluded since it is known that the 2-methyl-2-propanol reaction complex with $NO^+$, $(CH_3)_3CO(H)–NO^+$ (i.e., protonated *tert*-butyl nitrite, vide supra) decomposes exclusively to *tert*-$C_4H_9{}^+$ and HONO [14].

As already mentioned, the 1-butyl cation does not exist and therefore a rearrangement of the 1-butyl moiety in protonated 1-nitrobutane is necessary in order that a stable butyl cations can be formed during the dissociation of $C_4H_9NO_2{\cdot}H^+$. The energy requirement for such an isomerization, regardless as to whether the nitro-to-nitrite rearrangement occurs, is the probable reason why protonated 1-nitrobutane dissociates only slowly in comparison with protonated 2-methyl-2-nitrobutane. This reactivity is generally in agreement with previously observed unimolecular chemistry of protonated 1-nitropropane, 2-nitropropane and 2-methyl-2-nitropropane obtained using methane chemical ionisation, CI [30].

An interesting aspect of this protonation ion chemistry relates to the reactivity of the product ions with water molecules. When water vapour is added to the helium carrier gas of the SIFT instrument, $MH^+{\cdot}(H_2O)_{1,2,3}$ ions form via sequential three-body association reactions such as:

$$M \cdot H^+ + H_2O \xrightarrow{He} M \cdot H_3O^+ \quad (5a)$$

$$M \cdot H_3O^+ + H_2O \xrightarrow{He} M \cdot H^+(H_2O)_2 \quad (5b)$$

$$M \cdot H^+(H_2O)_2 + H_2O \xrightarrow{He} M \cdot H^+(H_2O)_3 \quad (5c)$$

The stabilising ‘third bodies’ are the helium atoms of the carrier gas, as indicated. This association occurred without exception for all the (protonated) molecules included in this study. A typical mass spectrum, in this case involving nitromethane, is shown in Fig. 2. As mentioned in Section 1, it is unusual for protonated organic molecules to form trihydrate ions, $MH^+(H_2O)_3$, at 300 K. However. As can be seen in Fig. 2, nitroalkanes do have this capability.

The rate coefficients of the three-body association reactions of the $M{\cdot}H^+$ ions with $H_2O$ molecules were determined by adding controlled amounts of water vapour to the helium carrier gas while simultaneously observing the loss of the $H_3O^+$ precursor ions and the production of $H_3O^+{\cdot}H_2O$ ions due to the analogous association reaction:

$$H_3O^+ + H_2O \xrightarrow{He} H_3O^+ \cdot H_2O \quad (6)$$

From such data, the rate coefficient for the association reactions (5a) have been estimated from the known rate coefficient for reaction (6), which is $5.8 \times 10^{-28}$ cm$^6$ s$^{-1}$ at 298 K [41] under these SIFT conditions (helium pressure of 100 Pa at a temperature of 300 K). The three-body rate coefficients relevant to the present study are given in Table 4. It can be seen that these association reactions are several times faster than reaction (6).

Another type of secondary ion chemistry that may occur involves the reactions of the ion products of the primary reac-

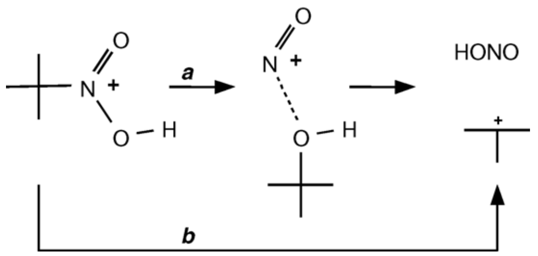

Scheme 2. Two possible pathways (a) and (b) for the fragmentation of protonated *tert*-butyl nitrite to *tert*-$C_4H_9{}^+$ and HONO.

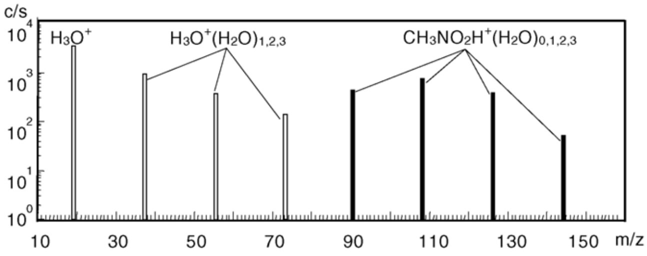

Fig. 2. A SIFT–MS spectrum obtained using $H_3O^+$ precursor ions for nitromethane in the presence of water vapour.

Table 4
Three-body rate coefficients for the association reactions of protonated nitroalkanes with water in He carrier gas at 300 K

| Reaction | $k_3$ (cm$^6$ s$^{-1}$) |
|---|---|
| $CH_3NO_2 \cdot H^+ + H_2O \rightarrow^{He} CH_3NO_2 \cdot H_3O^+$ | $1.1 \times 10^{-27}$ |
| $C_2H_5NO_2 \cdot H^+ + H_2O \rightarrow^{He} C_2H_5NO_2 \cdot H_3O^+$ | $3.6 \times 10^{-27}$ |
| $C_3H_7NO_2 \cdot H^+ + H_2O \rightarrow^{He} C_3H_7NO_2 \cdot H_3O^+$ | $4.7 \times 10^{-27}$ |
| $(CH_3)_2CHNO_2 \cdot H^+ + H_2O \rightarrow^{He} (CH_3)_2CHNO_2 \cdot H_3O^+$ | $1.1 \times 10^{-26}$ |

The uncertainty is ±25%.

tions with neutral nitroalkane molecules. Thus, it is seen that protonated ions of nitromethane associate with their neutral parent molecules to form proton-bound dimers:

$$CH_3NO_2 \cdot H^+ + CH_3NO_2 \xrightarrow{He} (CH_3NO_2)_2 \cdot H^+ \tag{7}$$

The $(CH_3)_2COH^+$ ion product of reaction (2b) also associates with neutral parent molecules in a three-body reaction:

$$(CH_3)_2COH^+ + (CH_3)_2CHNO_2 \xrightarrow{He} C_3H_7NO_2 \cdot C_3H_7O^+ \tag{8}$$

The $C_4H_9{}^+$ ions produced in the 2-methyl-2-nitropropane reaction (note that it is also a product of the $NO^+$ and $O_2{}^{+\bullet}$ reaction, see Table 3 and below) react further with neutral 2-methyl-2-nitropropane:

$$C_4H_9{}^+ + C_4H_9NO_2 \xrightarrow{He} C_4H_9NO_2 \cdot C_4H_9{}^+;\ 27\% \tag{9a}$$

$$C_4H_9{}^+ + C_4H_9NO_2 \rightarrow C_4H_9NO_2H^+ + C_4H_8;\ 6\% \tag{9b}$$

$$C_4H_9{}^+ + C_4H_9NO_2 \rightarrow (C_4H_8)_2NO^+ + H_2O;\ 7\% \tag{9c}$$

$$C_4H_9{}^+ + C_4H_9NO_2 \rightarrow C_4H_8NO_2{}^+ + C_4H_{10};\ 10\% \tag{9d}$$

$$C_4H_9{}^+ + C_4H_9NO_2 \rightarrow C_4H_8NO^+ + C_4H_9OH;\ 50\% \tag{9e}$$

The butyl cation involved in reaction (9) is actually a protonated "isobutene" having a proton affinity of 802.1 kJ/mol. The proton transfer reaction (9b) is therefore 12 kJ/mol endothermic and thus parallel association (9a) can occur.

### 3.4. The $NO^+$ reactions

The reactions of $NO^+$ with the nitroalkanes included in this study are all three-body association reactions forming $M{\cdot}NO^+$ adduct ions:

$$NO^+ + M \xrightarrow{He} M \cdot NO^+ \tag{10}$$

Note that HNO formation by hydride ion transfer is endothermic in all these reactions and hence it is not observed. The effective binary rate coefficients, $k_{2\mathrm{eff}}$, of these three-body reactions (see Table 2) are less than their collisional rate coefficients, but they increase with increasing size of M, as the lifetime of the reaction complex $(M{\cdot}NO^+)^*$ increases allowing for its more efficient stabilization in collisions with the He atoms. For the isomers on nitrobutane the $k_{2\mathrm{eff}}$ are within experimental error equal to $k_c$.

It was interesting to observe that the adduct ions of these reactions further associate with their parent molecules, M, to form $NO^+$ bound dimers analogous to the proton-bound dimer mentioned previously:

$$M \cdot NO^+ + M \xrightarrow{He} (M)_2 \cdot NO^+ \tag{11}$$

Similar dimer ions have been observed previously in a study of the correlation of $NO^+$ affinity with proton affinity [42]. The binding energy of nitromethane to $NO^+$ was also determined by equilibrium studies in high pressure mass spectrometer (HPMS) as 25.2 kcal/mol = 105.4 kJ/mol [43] together with the binding energy of a second nitromethane molecule (i.e., exothermicity of reaction (11) for the case of nitromethane) 19.5 ± 1.3 kcal/mol.

The nitrobutane reactions are an exception to this reactivity pattern, since $NO_2$ abstraction from the neutral reactant occurs forming the $C_4H_9{}^+$ ion and $N_2O_3$ as a neutral product. This is the only reaction process that occurs in the 2-methyl-2-nitropropane reaction:

$$NO^+ + (CH_3)_3CNO_2 \rightarrow (CH_3)_3C^+ + N_2O_3 \tag{12}$$

This reaction is exothermic by 57 kJ/mol. In the 1-nitrobutane reaction a minor (15%) $NO_2$ abstraction channel occurs in parallel with the major three-body association channel. Secondary reactions of the $C_4H_9{}^+$ product of reaction (12) with the neutral parent molecule followed the reactions (9a)–(9e). Therefore its structure is the same as the structure of the product ion of the $H_3O^+$ reaction (4b).

### 3.5. The $O_2{}^{+\bullet}$ reactions

The parent radical cation is the major product of the $O_2{}^{+\bullet}$ reaction with the smallest molecule, nitromethane, together with a minor $NO^+$ formation channel:

$$O_2{}^{+\bullet} + CH_3NO_2 \rightarrow CH_3NO_2{}^{+\bullet} + O_2;\ 90\% \tag{13a}$$

$$O_2{}^{+\bullet} + CH_3NO_2 \rightarrow NO^+ + CH_3O^\bullet + O_2;\ 10\% \tag{13b}$$

Reaction (13a) is exothermic by 103 kJ/mol and reaction (13b) by 131 kJ/mol. It has been suggested previously in a study involving charge transfer from $N^{2+}$ to $CH_3NO_2$ [43] that dissociation of excited $CH_3NO_2{}^{+\bullet}$ to $NO^+$ and $CH_3O$ proceeds via a prior isomerization of $CH_3NO_2$ to $CH_3ONO$ requiring ~80 kJ/mol.

The parent radical cation formed in reaction (13a) reacts with $CH_3NO_2$ and a secondary methylated nitromethane ion $CH_3NO_2CH_3{}^+$ is formed together with a neutral $NO_2$:

$$CH_3NO_2{}^{+\bullet} + CH_3NO_2 \rightarrow CH_3NO_2 \cdot CH_3{}^+ + NO_2{}^\bullet \tag{14}$$

The same ion at *m*/*z* 76 can be prepared by the self-CI of nitromethane [44,45]. The CAD mass spectra (see Section 2.2) of this ion are consistent with the structure of oxygen-methylated nitromethane, since the two most abundant fragment ions in the spectra, *m*/*z* 45 and *m*/*z* 30, correspond to the loss of a methoxy radical followed by the loss of a methyl radical. This fragmentation scenario was corroborated using deuterated nitromethane-$d_3$ when the peak at $m/z$ 45 shifted to $m/z$ 48 whilst the $m/z$ 30 remained unchanged. Reaction (14), formally being of $S_N2$ type, was calculated to be 211 kJ/mol exothermic at the B3LYP/6-31+G(d,p) level of theory. Note that the $CH_3NO_2^{+\bullet}$ product is quite reactive and forms protonated methanol on reaction with water vapour molecules:

$$CH_3NO_2^{+\bullet} + H_2O \rightarrow CH_3OH_2^{+} + NO_2^{\bullet} \qquad (15)$$

It is important to be aware of this when attempting to analyse nitromethane in humid air samples by SIFT–MS using $O_2^{+\bullet}$ precursor ions. Note that the other product ions of the $O_2^{+\bullet}$ reactions listed in Table 3 do not react with $H_2O$ molecules.

In all the reactions of $O_2^{+\bullet}$ with the larger nitroalkanes charge transfer is followed by fragmentation via $NO_2$ elimination producing a single hydrocarbon ion:

$$O_2^{+\bullet} + C_2H_5NO_2 \rightarrow C_2H_5^{+} + NO_2^{\bullet} + O_2 \qquad (16)$$

Therefore, a secondary reaction analogous to reaction (14) was not observed. Similar trends can be seen in the electron ionisation (EI) spectra of nitroalkanes [46] where the parent molecular ion is observed only for nitromethane and is absent from the EI spectra of the larger nitroalkanes.

The hydrocarbon ions formed in the other five reactions react with the parent molecules either by proton transfer association:

$$C_2H_5^{+} + C_2H_5NO_2 \rightarrow C_2H_5NO_2 \cdot H^{+} + C_2H_4 \qquad (17)$$

or by proton transfer and parallel three-body association, as in the reaction of 1-nitropropane:

$$C_3H_7^{+} + C_3H_7NO_2 \xrightarrow{He} C_3H_7NO_2 \cdot C_3H_7^{+};\ 10\% \qquad (18a)$$

$$C_3H_7^{+} + C_3H_7NO_2 \rightarrow C_3H_7NO_2 \cdot H^{+} + C_3H_6;\ 90\% \qquad (18b)$$

The reaction of 2-nitropropane is similar, the branching fraction of three-body association being lower at 5%. Competition between these two processes indicates that the proton affinities of $C_3H_6$ (751.6 kJ/mol [22]) and of $C_3H_7NO_2$ are similar, which supports our ab initio results given in Table 1.

The only ion product of the $O_2^{+\bullet}$ reactions of both nitrobutane isomers is $C_4H_9^{+}$. This ion undergoes secondary chemistry as described by reaction (9a)–(9e), which is identical to reactivity of the product of reaction (4b). This again indicates that the $C_4H_9^{+}$ ion, which is the common product of all three precursor ion reactions, has the same structure in all these three cases.

## 4. Concluding remarks

The data obtained in this study indicate that SIFT–MS analyses of nitroalkanes are feasible even in presence of water vapour. The combination of the three different precursor ions used for SIFT–MS provides a tool for the positive identification of the nitroalkanes in mixtures of volatile compounds in air. The ion products of the nitroalkane reactions have a propensity to form cluster ions. Protonated molecules $MH^{+}$ can bind up to three water molecules under the conditions of these SIFT experiments. The secondary ion chemistry of protonated molecules with the parent molecules also proceeds via cluster formation (association). $MH^{+}$ ions, whether they are formed in primary proton transfer reactions of $H_3O^{+}$ or in secondary reactions of some of the product ions of the $O_2^{+\bullet}$ reactions associate with the parent molecules forming proton-bounded dimers:

$$C_3H_7NO_2 \cdot H^{+} + C_3H_7NO_2 \xrightarrow{He} C_3H_7NO_2 \cdot H^{+} \cdot C_3H_7NO_2 \qquad (19)$$

The calculated proton affinities of the compounds are quite consistent with the experimental observations. The rate coefficients of the primary reaction of $O_2^{+\bullet}$ are all close to collisional, with the exception of nitromethane. The measured rate coefficients and the identified primary products together with the secondary products of their reactions with $H_2O$ represent a valuable addition to SIFT–MS kinetic library.

## Acknowledgements

We are very grateful to Professor David Smith FRS for discussions and for reading the manuscript. We gratefully acknowledge financial support by the Grant Agency of the Czech Republic (project numbers 202/03/0827 and 203/02/0737).

## References

[1] IARC Monographs on the Evaluation of the Carcinogenic Risk of Chemicals to Humans, 29 (1982) 331.

[2] C.J. Smith, T.A. Perfetti, R. Garg, C. Hansch, Food Chem. Toxicol. 41 (2003) 807.

[3] G. Petrelli, G. Siepi, L. Miligi, P. Vineis, Scand. J. Work. Environ. Health 19 (1993) 63.

[4] K. Sakano, Sh. Oikawa, M. Murata, Y. Hiraku, N. Kojima, Sh. Kawanishi, Mutat. Res. 479 (2001) 101.

[5] International Programme on Chemical Safety, 2-Nitropropane, Environmental Health Criteria (EHC) Monographs, 138, World Health Organization, Geneva 1992. available on-line: http://www.inchem.org/documents/ehc/ehc/ehc138.htm.

[6] Occupational Safety & Health Administration, Occupational Safety & Health Standards, US Department of Labor, 1997.

[7] D. Smith, P. Španel, in: J. Lindon, G. Tranter, J. Holmes (Eds.), Encyclopedia of Spectroscopy, Spectrometry, Mass Spectrometry, Academic Press, London, 1999, available on-line: http://dx/, doi: org/10.1006/rwsp.2000.0278.

[8] P. Španěl, D. Smith, Int. J. Mass Spectrom. Ion Process. 167–168 (1997) 375.
[9] E. Arijs, Ann. Geophys. 1 (1983) 149.
[10] P. Španěl, T. Wang, D. Smith, Int. J. Mass Spectrom. 218 (2002) 227.
[11] P. Španěl, D. Smith, J. Phys. Chem. 99 (1995) 15551.
[12] P. Španěl, Y. Ji, D. Smith, Int. J. Mass Spectrom. Ion Process. 165–166 (1997) 25.
[13] P. Španěl, J.M. Van Doren, D. Smith, Int. J. Mass Spectrom. 213 (2002) 163.
[14] P. Španěl, D. Smith, Int. J. Mass Spectrom. Ion Process. 167–168 (1997) 375.
[15] P. Španěl, D. Smith, Int. J. Mass Spectrom. Ion Process. 172 (1998) 137.
[16] P. Španěl, D. Smith, Rapid Comm. Mass Spectrom. 14 (2000) 1898.
[17] S.M. Abbott, J.B. Elder, P. Španěl, D. Smith, Int. J. Mass Spectrom. 228 (2003) 655.
[18] D. Smith, N.G. Adams, Adv. Atom. Mol. Phys. 24 (1987) 1.
[19] D. Smith, P. Španěl, J.M. Thompson, B. Rajan, J. Cocker, P. Rolfe, Appl. Occup. Environ. Hyg. 13 (1998) 817.
[20] P. Španěl, D. Smith, Med. Biol. Eng. Comput. 34 (1996) 409.
[21] D. Smith, A.M. Diskin, Y. Ji, P. Španěl, Int. J. Mass Spectrom. 209 (2001) 81.
[22] E.P. Hunter, S.G. Lias, in: W.G. Mallard, P.J. Linstrom (Eds.), Proton Affinity Evaluation in NIST Chemistry WebBook, NIST Standart Reference Database Number 69, March 2003, National Institute of Standards and Technology, Gaithersburg, MD, 20899, available on-line: http://webbook.nist.gov/.
[23] G. Bouchoux, J.Y. Salpin, D. Leblanc, Int. J. Mass Spectrom. Ion Process. 153 (1996) 37.
[24] T. Su, W.J. Chesnavich, J. Chem. Phys. 76 (1982) 5183.
[25] D.R. Lide (Ed.), CRC Handbook of Chemistry and Physics, CRC, Boca Raton, 1991.
[26] M.J. Frisch, G.W. Trucks, H.B. Schlegel, G.E. Scuseria, M.A. Robb, J.R. Cheeseman, V.G. Zakrzewski, J.A. Montgomery, R.E. Stratmann, J.C. Burant, S. Dapprich, J.M. Millam, A.D. Daniels, K.N. Kudin, M.C. Strain, O. Farkas, J. Tomasi, V. Barone, M. Cossi, R. Cammi, B. Mennucci, C. Pomelli, C. Adamo, S. Clifford, J. Ochterski, G.A. Petersson, P.Y. Ayala, Q. Cui, K. Morokuma, D.K. Malick, A.D. Rabuck, K. Raghavachari, J.B. Foresman, J. Cioslowski, J.V. Ortiz, B.B. Stefanov, G. Liu, A. Liashenko, P. Piskorz, I. Komaromi, R. Gomperts, R.L. Martin, D.J. Fox, T. Keith, M.A. Al-Laham, C.Y. Peng, A. Nanayakkara, C. Gonzalez, M. Challacombe, P.M.W. Gill, B.G. Johnson, W. Chen, M.W. Wong, J.L. Andres, M. Head-Gordon, E.S. Replogle, J.A. Pople, Gaussian 98 (Revision A.1), Gaussian Inc., Pittsburgh PA, 1998.
[27] A.D. Becke, J. Chem. Phys. 98 (1993) 5648.
[28] G. Rahut, P. Pulay, J. Phys. Chem. 99 (1995) 14572.
[29] L.A. Curtiss, K. Raghavachari, J.A. Pople, J. Chem. Phys. 98 (1993) 1293.
[30] O.S. Chizhov, V.I. Kadentsev, G.G. Palmbach, K.I. Burstein, S.A. Shevelev, A.A. Feinsilberg, Org. Mass Spectrom. 13 (11) (1978) 611.
[31] M. Polášek, F. Tureček, J. Phys. Chem. A 103 (1999) 9241.
[32] G.I. Mackay, S.D. Tanner, A.C. Hopkinson, D.K. Bohme, Can. J. Chem. 57 (1979) 1518.
[33] G.I. Mackay, D.K. Bohme, Int. J Mass. Spectrom. Ion Proc. 26 (1978) 327.
[34] S.G. Lias, in: P.J. Linstrom, W.G. Mallard (Eds.), Ionization Energy Evaluation in NIST Chemistry WebBook, NIST Standard Reference Database Number 69, March 2003, National Institute of Standards and Technology, Gaithersburg MD, 20899, available on-line: http://webbook.nist.gov/.
[35] H.M. Rosenstock, K. Draxl, B.W. Steiner, J.T. Herron, J. Phys. Chem. Ref. Data 6 (Suppl. 1) (1977).
[36] V. Baranov, S. Petrie, D.K. Bohme, J. Am. Chem. Soc. 118 (1996) 4500.
[37] A. Cunje, C.F. Rodriquez, D.K. Bohme, A.C. Hopkinson, J. Phys. Chem. A 102 (1998) 478.
[38] A.J. Chalk, L. Radom, J. Am. Chem. Soc. 121 (1999) 1574.
[39] G. de Petris, Org. Mass Spectrom. 25 (1990) 557.
[40] S. Sieber, P. Buzek, P.v.R. Schleyer, W. Koch, J.W. de M. Carneiro, J. Am. Chem. Soc. 115 (1993) 259.
[41] D. Smith, P. Španěl, Rapid Comm. Mass Spectrom. 15 (2001) 563.
[42] F. Cacace, G. de Petris, F. Pepi, Proc. Natl. Acad. Sci. U.S.A. 94 (8) (1997) 3507.
[43] H. Wincel, Chem. Phys. Lett. 292 (1998) 193.
[44] M. Vairamani, Org. Mass Spectrom. 25 (1990) 271.
[45] L.E. Ramos, A.M. Fernandes, A.J. Ferrer Coreira, N.M.M. Nibbering, Int. J. Mass. Spectrom. 222 (2003) 101.
[46] S.E. Stein, in: P.J. Linstrom, W.G. Mallard (Eds.), Mass Spectra in NIST Chemistry WebBook, NIST Standard Reference Database Number 69, March 2003, National Institute of Standards and Technology, Gaithersburg MD, 20899, available on-line: http://webbook.nist.gov/.
[47] M.J.S. Dewar, M. Shanshal, S.D. Worley, J. Am. Chem. Soc. 91 (1969) 3590.